geosciences

MDPI

Article

Evaluation of the Installation Effect on the Performance of a Granular Column

Firas Ghrairi, Arash Alimardani Lavasan *,† and Torsten Wichtmann

Chair of Soil Mechanics, Foundation Engineering and Environmental Geotechnics, Ruhr-Universität Bochum, Universitätsstr. 150, 44780 Bochum, Germany; firas.ghrairi@rub.de (F.G.); torsten.wichtmann@rub.de (T.W.)
* Correspondence: arash.alimardanilavasan@rub.de
† Candidate University of Baghdad.

Abstract: The procedure of granular column installation impacts soil properties such as stress state, stiffness, and permeability in the near-field of the column. For an accurate and efficient design of relatively costly geostructures on improved subsoil with granular columns, a reliable estimation of the column installation effects on the properties of natural subsoil deposits is necessary. To achieve this goal, two phases are adopted in numerical simulations: (1) the installation phase based on the cavity expansion method using a 2D model, and (2) the construction phase in conjunction with the improved soil properties after column installation using a 3D model. The latter phase includes the construction of an embankment and the column is considered as an independent unit. The soil profile, i.e., stress and stiffness, is spatially updated from the first simulation (i.e., installation phase). In this frame, the stiffness was calculated according to a procedure suggested by the authors to determine the final stiffness based on the formulation of the Hardening Soil constitutive model. The numerical models were validated through a comparison with the recorded data of a field test obtained from the Klagenfurt site. Results of numerical analyses for the case study indicated that application of proposed methodology led to a more accurate estimate of the settlement, demonstrating that the installation effects have be taken into consideration to assure reliable evaluation of granular-column performance.

Keywords: granular column; installation effect; settlement; numerical modeling; soil property evolution

Citation: Ghrairi, F.; Alimardani Lavasan, A.; Wichtmann, T. Evaluation of the Installation Effect on the Performance of a Granular Column. *Geosciences* **2022**, *12*, 216. https://doi.org/10.3390/geosciences12050216

Academic Editors: Mohamed Shahin and Jesus Martinez-Frias

Received: 28 March 2022
Accepted: 29 April 2022
Published: 18 May 2022

1. Introduction

Granular columns are among the most economical and scientific solutions for dealing with weak soil. This technique has been used since 1950. The principle idea of this technique is to relieve the load on soft soils and concentrate it on the column due to the high stiffness of the column material. Granular columns are intended to improve bearing capacity, decrease settlement, speed up consolidation by providing an additional drainage path, and prevent soil liquefaction. Granular columns are constructed by the displacement or replacement of unsuitable native soil with granular material. The construction of granular columns in weak soil is not just soil material replacement but also has an accompanying effect represented via vibration and horizontal displacement [1]. The installation of the granular column procedure impacts soil properties such as stiffness, permeability, and stress state within the area near the column. Over the last few decades, a significant number of field and laboratory tests have been conducted to study the effect of granular column installation on the properties of natural soils. Some of these effects, such as increases in pore pressure and horizontal stresses, have been observed in field studies [2–4]. The destructuration (i.e., degradation of structure upon plastic straining) of the surrounding soil was also observed due to the vibration effect during the installation. According to [5], these measurements are related to a specific case; therefore, the conclusion obtained cannot be generalized. The reason for this finding may be that the installation impact is influenced by a variety of factors, including soil type, installation technique (replacement

or displacement), column diameter, etc. The author of [2] investigate the changes in stress and stiffness of subsoil during the installation of granular columns, where an increase in the earth pressure coefficient value and the stiffness of almost 1.70 and 2.5 times of the initial values were observed, respectively.

The numerical method has also been used to investigate these effects. The installation effect can be considered by applying various methods such as increasing the lateral earth pressure coefficient (K) and considering that the column is "wished in place". This assumption is followed by Priebe [6], who suggested using an earth pressure coefficient equal to 1.0 in the vicinity of the column. Nevertheless, other researchers proposed using different values of the lateral earth pressure coefficient (K) in accordance with different hypotheses [1,7,8].

Another popular approach to address the installation effect was based on the cavity expansion method (CEM) to mimic the expansion of the radial ground movements during the installation procedure. The general concept of the CEM was first introduced by [9], who described a theoretical method for calculating the required pressure to enlarge a spherical and cylindrical hole in a strain-hardening material (i.e, the strengthening of a material during large strain deformation). Due to its simple simulation method and numerical stability, this method is considered to be one of the most popular methods, according to [2]. To model this process, the majority of numerical studies about granular column installations in the literature adopted the cavity expansion method [2,5,10–12].

Among various studies, [11] studied the impact of column installation on the lateral earth pressure coefficient (K) around the columns and the impact of the updated K value on the settlement improvement factors in subsoil enhanced with granular columns. The author developed a cavity expansion model for a single column in accordance with the unit cell approach. The unit cell approach is used to represent a single column inside an infinitely large number of granular columns. The approach refers to a column with regular spacing between adjacent columns that is supported by a rigid raft or a large evenly loaded region, such as an embankment supported on soft soils. The effective diameters for triangular, square, and hexagonal patterns of granular columns were $1.05S$, $1.13S$, and $1.29S$, respectively, where S refers to the column spacing. Two scenarios were considered in conjunction with the unit cell approach to evaluate the load-settlement behavior of the soil–granular column system. In the primary scenario, the earth pressure coefficient was assumed to remain unaffected by column installation (i.e., $K = 1 - sin\phi'$). In contrast, a post-installation K profile was applied in the second scenario based on the cavity expansion theory. The results showed a significant increase in the improvement factor when the influence of the installation effect on the earth pressure coefficient was considered. Therefore, they recommended using this method as an alternative to the conventional "wished in place" column installation technique that assumes immediate activation of the column in the model without any lateral ground movements.

In 2013, ref. [13] employed the cavity expansion method to simulate the granular column installation process. The analysis was carried out using the finite element Plaxis software. By applying prescribed displacement technique, the cavity expanded from an initial radius of 0.10 m to the final column radius of 0.50 m that showed an increase in horizontal stress was 3.20 times the initial value. In case of granular column installation in structured natural clay deposits, ref. [14] studied the effect of granular column installation on the performance of the foundation system in Bothkennar structured clay, where the theory of cavity expansion was applied, as well. They finally concluded that the earth pressure coefficient could rise up to about 1.60 times the initial value near the column and decrease gradually with distance to get close to its original value after about five times the column diameter ($5d_c$). A similar dramatic increase in soil stiffness after consolidation was considered as a consequence of pore pressure increase upon installation. Additionally, it was observed that the effect can extend up to six times the column diameter while it reaches a peak of 2.6 times the initial soil stiffness. They also discovered that considering the installation effect allows for the proper investigation of the bearing capacity up to a

35% increase and the settlement up to a 45% reduction. In this study, the evolution of the stiffness was assessed according to the equation suggested by [15]. The proposed correlation is based on experimental results from the triaxial test on sand soil and numerical work using the elastic perfectly plastic Mohr–Coulomb model to estimate the enhanced soil stiffness value from the change in the mean effective stress, and the equation is limited to a low strain level.

In practice, the design of granular columns is often based on flexible or rigid inclusion assumption, while the impact on the surrounding soil induced by the installation of the columns is not generally taken into consideration during the design process [5]. For a proper design of geostructures on soft subsoils enhanced with granular columns, a reliable prediction of the installation effects of columns on the properties of the natural deposits is necessary because that is the only way to allow accurate prediction of system.

The main aim of this study is to determine the impact of column installation in weak soils, which is represented by soil stress state and stiffness characteristics that can be used in finite-element simulations, rather than assuming or conducting rigorous laboratory testing, which requires significant time and expense, as well as multiple efforts, by proposing a procedure for calculating the change in stress regime and soil stiffness. To achieve this objective, the present study proposed a numerical approach to sequentially simulate the installation and construction phases through two calculation models. In this approach, the installation process and its impacts on the adjacent soils are investigated through a simplified and computationally robust model. The construction phase that accounts for the set-up of infrastructure (e.g., road, founded buildings, etc.) is modelled through a sophisticated model in which the stress field and soil parameters in the vicinity of the column are defined in accordance with the results obtained from the installation model. The proposed approach was validated and its advantages highlighted based on the data monitored in the Klagenfurt field test in Austria [16].

2. Methodology

As mentioned before, simulation of the column installation in the construction model with the complicated geometry including several granular columns is computationally impossible [17,18]. For instance, modelling the construction stage immediately after column installation is inconvenient due to the highly deformed mesh and possible inadequacy of boundary conditions [17]. As a result, it was thought acceptable to represent the problem separately. The division of the model into two models would help to reduce the computational effort and to split the dimensional complexity of the models for the rather 2D installation of a single column and construction of the infrastructure on a large number of columns that often requires a 3D simulation procedure. In this study, effects of column installation on soil state variables were investigated in a 2-dimensional axisymmetric model, while the obtained post-installation soil parameters and stress field were transferred to the construction model as predefined initial conditions. The process to transmit data (internal variables, state variables, and stress states) from the installation model to the construction model is important in this scenario. This concept is illustrated in Figure 1. The earth pressure coefficients after installation (K_r) were represented by the changes in radial stresses, while the vertical stresses remained unchanged. These values formed the installation model and were incorporated into the initial stress generation phase of the construction stage model.

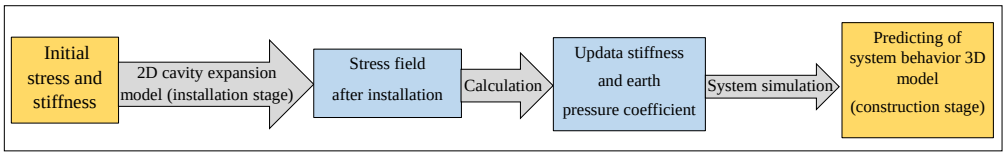

Figure 1. Steps adopted to calculate the stress state and the stiffness in this study.

After evaluation of the changes in the stresses upon column installation, the post-installation stiffness (E_{50}, E_{oed}, and E_{ur}) from the installation stage were calculated according to the Hardening Soil (HS) model formulation. The challenge at this stage was to correlate the stiffness at the post-installation stress field to the stiffness components at a reference pressure (E_{50}^{ref}, E_{oed}^{ref}, and E_{ur}^{ref}) as the construction model's input. The methodology adopted in the literature to calculate the reference stiffness values is illustrated in Figure 2. The approach is based on the fact that changes in stress results in stiffness evolution [19]. To obtain the stiffness values at reference pressure, two steps were followed:

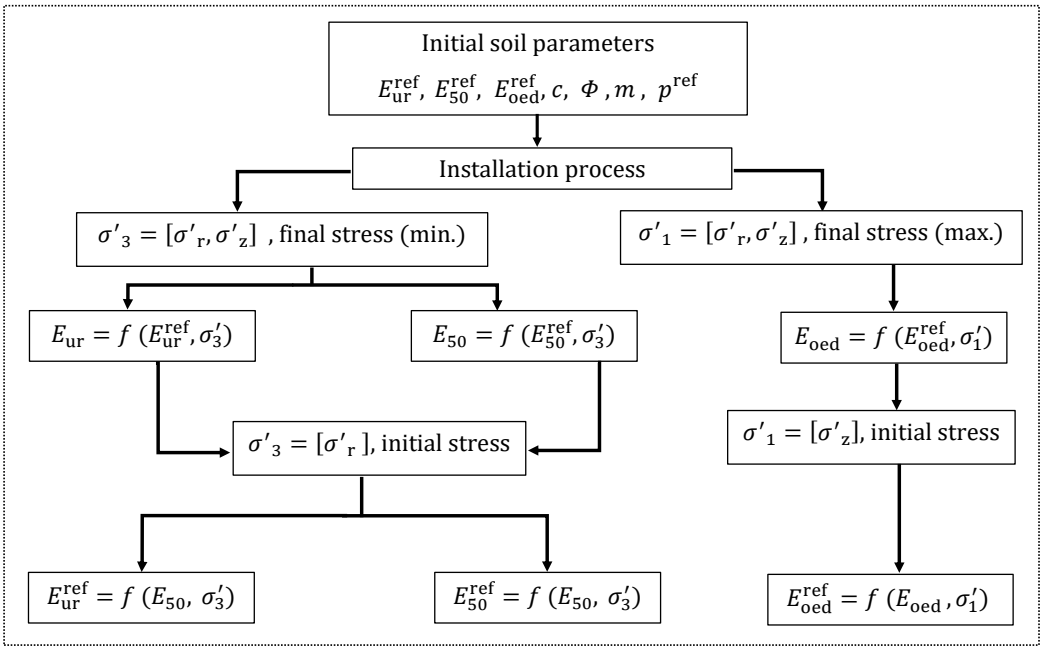

Figure 2. Flow chart for stiffness calculation.

1. As the secant stiffness E_{50} for primary loading is minor-principal-stress-dependent in hardening soil model, the E_{50} can be calculated as:

$$E_{50} = E_{50}^{ref} \cdot \frac{(c \cdot cos\phi - \sigma_3' \cdot sin\phi)}{(c \cdot cos\phi + p^{ref} \cdot sin\phi)}^{m} \quad (1)$$

   where E_{50}^{ref} is the constitutive parameter at reference pressure and E_{50} states the postinstallation stiffness at current minor principal stress σ_3' which is defined as the minimum value of σ_r' and σ_z' after installation. In the same way, E_{ur}^{ref} and E_{oed}^{ref} are calculated. However, according to the HS model, the E_{oed}^{ref} is dependent upon the major principal stress σ_1' that reads the maximum value of σ_r' and σ_z'.
2. The stiffness at the reference pressure that corresponds to post-installation stiffness can be obtained according to the initial geostatic stresses σ_r' or σ_z' and the stiffness calculated in the previous calculation step according to the HS model Equation (2):

$$E_{50}^{ref} = E_{50} / \frac{(c \cdot cos\phi - \sigma_3' \cdot sin\phi)}{(c \cdot cos\phi + p^{ref} \cdot sin\phi)}^{m} \quad (2)$$

   In the same way, E_{oed}^{ref} and E_{ur}^{ref} are calculated to be adopted in the second model.

2.1. Numerical Models

The commercially available finite element Plaxis software was used to create the numerical model in this work. The models developed in the frame of the present study were (a) a 2D model corresponding to the installation phase based on the unit cell approach and (b) a 3D model corresponding to the construction step, see Figure 3. The 2D axisymmetric model aimed to compute the post-installation stress and stiffness by simulating the ground movements induced by installation procedure for a single column. In this frame, the 3D model was to assess the system's behaviour (i.e., soil–column–geostructure interactions) during the construction (and even operation) of the infrastructure with reference to the installation model outcomes. In order to account for nonlinearity, stress dependency of the soil stiffness, and shear strength, the advanced Hardening Soil (HS) model was adopted in both 2D and 3D models to simulate the behaviour of soil and columns.

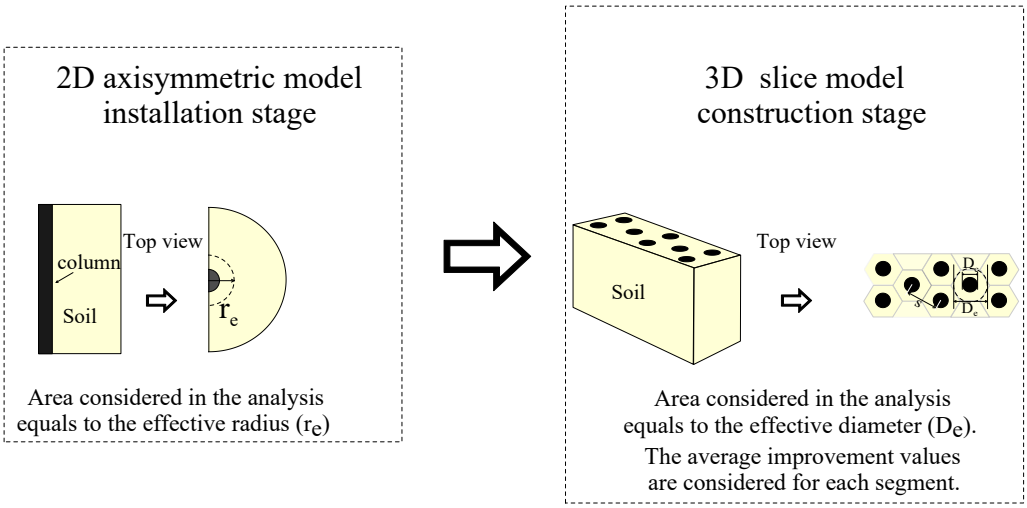

Figure 3. Details of the concept adopted in numerical model.

2.2. Mesh and Boundary Conditions

In the installation model, a two-dimensional axisymmetric model in conjunction with 15-noded elements was developed to simulate the column installation process. Depending on the column diameter, large lateral ground movements can take place due to the introduction of the column into the subsoil. This procedure was simulated through predefined lateral displacements at the boundaries of the expanded column based on the cylindrical cavity expansion theory.

The soil profile, column dimension, and parameters used in this model were taken from the Klagenfurt project [16] as illustrated in Table 1. The size of the model in horizontal direction was set to be 30 m, which is larger than two times the installed column length [5], to minimize the influence of the side boundaries, while the depth of the model was selected to be the same as the length of the column (i.e., 14.5 m) to avoid modeling the column tip, which can cause numerical instabilities, as mentioned by [5]. Figure 4a depicts the geometry of the numerical model for column installation as well as a schematic sketch of the subsoil stratigraphy. The boundary conditions for consolidation were set to be closed in all directions except the ground surface. This assumption imposed consolidation of the excess pore pressure through the granular columns.

Table 1. Soil parameters adopted by [16].

Symbol	Stone Columns	Clayey Silts	Sand Loose	Embankment
γ/γ_{sat} [kN/m^3]	20/23	16/19	18/21	22/22
E_{50}^{ref} [kN/m^2]	70,000	7500	16,000	35,000
E_{oed}^{ref} [kN/m^2]	70,000	5000	16,000	35,000
E_{ur}^{ref} [kN/m^2]	225,000	30,000	80,000	105,000
m [-]	0.3	1.0	0.55	0.5
p_{ref} [kN/m^2]	100	100	100	100
ϕ [°]	35	22.5	27.5	35
ν [-]	0.2	0.2	0.2	0.2
$c^{'}$ [kN/m^2]	0.1	10	0.1	10
ψ [°]	5	0	2	0

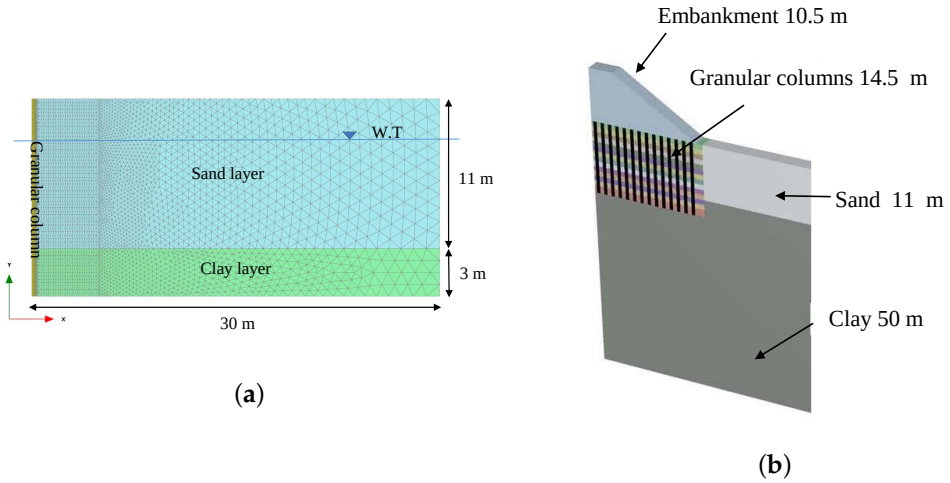

(**a**) (**b**)

Figure 4. Numerical models: (**a**) 2D installation model; (**b**) construction 3D model.

As shown in Figure 4b, the 3-dimensional construction model was in conjunction with 10-noded tetrahedral elements for the granular columns and soft soil. In order to enable transmission of the post-installation soil parameters in the near-field of column from 2D model to the 3D model, the subsoil in the construction model was divided into 1 m thick sublayers. In the 3D model, due to the plane strain nature of the problem and symmetry of the system along the road axis, only a half-system slice including three rows of columns in a triangular pattern under the embankment was simulated. The lateral extent of the model was chosen to be 110 m and the depth to be 50 m to avoid any influence from the outer boundaries. In the 3D construction model, the boundaries were fixed against normal movements, while no displacement restriction was applied to the model surface.

2.3. Modeling of Granular Column Installation

The cylindrical cavity expansion method, with the procedure suggested by [5,10,11], was used in the present study to simulate the lateral ground movements upon column installation. Since the rate of the column installation is significantly higher than the consolidation in subsoil, cavity expansion analysis was conducted assuming an undrained condition that was followed by a consolidation analysis to account for rapid pore pressure dissipation due to drainage influence of the column. In the present study, simulation of the installation process using a 2D axisymmetric model consisted of the following calculation phases:

1. The initial vertical stresses in the unimproved subsoil were determined by the soil unit weight γ and depth z ($\sigma_v = \gamma \cdot z$), whilst the horizontal stresses were defined as $\sigma_h = K_0 \cdot \sigma_v$, where $K_0 = 1 - (sin\phi)$ [20].

2. This phase dealt with the creation of a cylindrical hole with an initial radius of a_0 that was filled with the dummy material (pure elastic material with low stiffness) to avoid discontinuity during the following radial expansion process [10]. In reality, the cavity expands from zero to its final radius in case of vibroflotation column installation. In contrast, according to [5], it is necessary to start from a radius of a_0 to have a finite circumferential strain in the numerical simulation.
3. Applying the prescribed displacement from the initial radius to the final one along the entire column length, the main problem in modeling cavity expansion in an FEM framework is the amount of radial strain imposed in the model to mimic field conditions and, more critically, whether this expansion violates the FE theoretical assumptions [21]. Therefore, different displacement values were used (i.e., Δ_r = 0.05, 0.1, 0.15 m), along with different initial radius values (a_0 = 0.3, 0.25, and 0.20 m). The column radius (r_c) used was 0.35 m. Various expansion degrees have been investigated in order to determine the optimal degree of expansion cavity to obtain the necessary performance. In this research, the final column diameter was set at ($D_c = d_0 + 2\Delta_r$ = 0.7 m). Therefore, to satisfy three different degrees of applied expansion, the starting column diameter d_0 was (0.40, 0.5, and 0.6 m), representing the poker's diameter.
4. The dummy material inside the expanded column was substituted with the granular fill material in this phase to realistically simulate the interaction between the soil and granular column.
5. The consolidation stage was the final phase in this analysis which allowed for dissipation of the pore pressure induced during the installation process. At the end of this calculation phase, the final postinstallation stiffness and stress fields were achieved. Figure 5 shows the detailed geometry for each step.

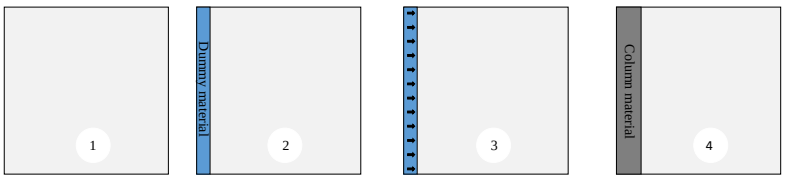

Figure 5. Calculation phase to simulate the column installation process: (**1**) initial phase; (**2**) create a hole and insert dummy; (**3**) applied displacement; (**4**) insert column material and consolidation.

3. Description of the Case Study

3.1. Klagenfurt Project

The Wörthersee stadium was built between 2006 and 2007 in preparation for the European Soccer Championship (EURO 2008) in Austria. The test field was located on the ramp area, which took visitors to the grandstand at the western end of Wörthersee stadium. In order to monitor the behavior of improved subsoil, this test field was well equipped with three multilevel piezometers (MLP), one multilevel extensometer (EX), one horizontal inclinometer (INCL), and several settlement gauges. Before the construction of the project, a cone penetration test, dynamic tests (DPH), and a seismic test were also carried out [16,22].

The construction of ramp was completed in six stages, in which the first and second layers, respectively, had a thickness of 1 m and 1.5 m and the third to sixth layers were 2 m thick. Table 2 illustrates the processes of ramp building and the consolidation period for each layer.

The subsoil in the ramp construction area consisted of loose-to-medium-dense lacustrine sand up to a depth of about 10–12 m that was underlaid by a soft lacustrine clay (i.e., clayey silts) that reached a depth of more than 50 m. The water table was measured at a depth of 3.1 m. Figure 6a depicts the subsoil stratigraphy.

The bottom-feed method was used to install the granular columns with a length of 14.5 m and diameter of 0.7 m in a triangular pattern, as shown in Figure 6b. Assuming

a height of 11 m for the lacustrine sand layer, 3.5 m of the column was assumed to be introduced into the soft clay layer.

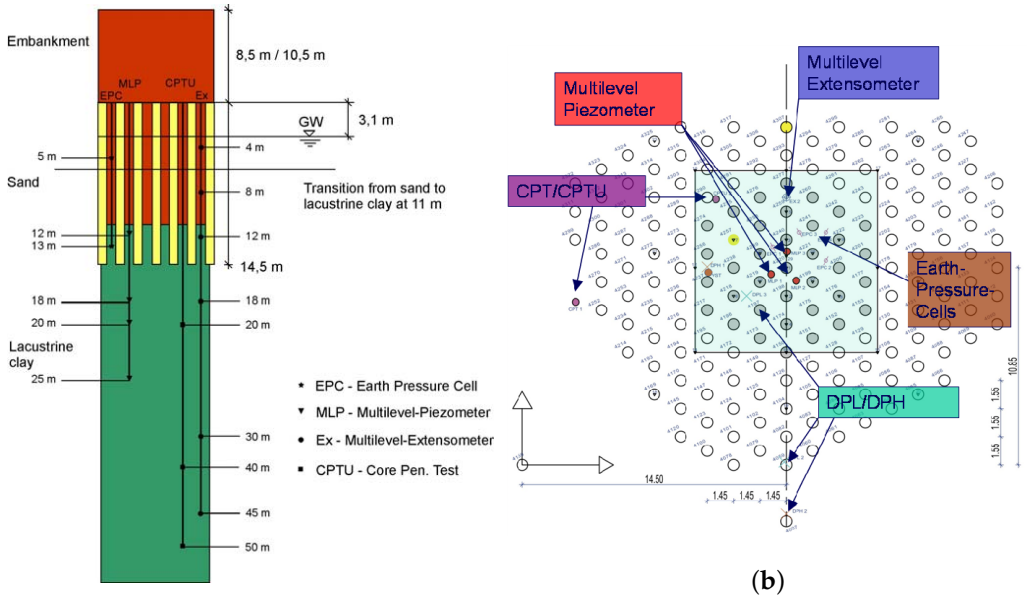

Figure 6. Details of Klagenfurt site. (**a**) Cross-section with soil layers and measuring devices; (**b**) plan view of arrangement of granular column and measuring device in field, ref. [16].

Table 2. Process of construction [16].

Phase No.	Phase	Time Total
1	Granular columns (Part 1)	2 days
2	No progress of construction	8 days
3	Granular columns (Part 2)	31 days
4	No progress of construction	36 days
5	Embankment height 1 m	43 days
5	Embankment height 2.5 m	51 days
5	Embankment height 4.5 m	65 days
6	No progress of construction	80 days
7	Embankment height 6.5 m	87 days
7	Embankment height 8.5 m	99 days
7	Embankment height 10.5 m	105 days
8	Last measurement	379 days

3.2. Field Measurement

The measurement devices installed in the ramp area allowed for a continuous monitoring of settlements and pore water pressure in the subsoil. For both construction phases (granular column installation and placement of a 10.5 m high ramp) and after 14 months of consolidation, the measurements were accessible at different depths. Figure 7a shows the settlements under the ramp obtained using various methods during the installation of the granular columns and the subsequent construction of the ramp, up to about 400 days.

The excess pore water pressure measurements were available at various depths. Three multilevel piezometers were installed at five different depths. The generation of excess pore water pressure at various depths during the installation of granular columns and after the ramp construction until 400 days is depicted in Figure 7b.

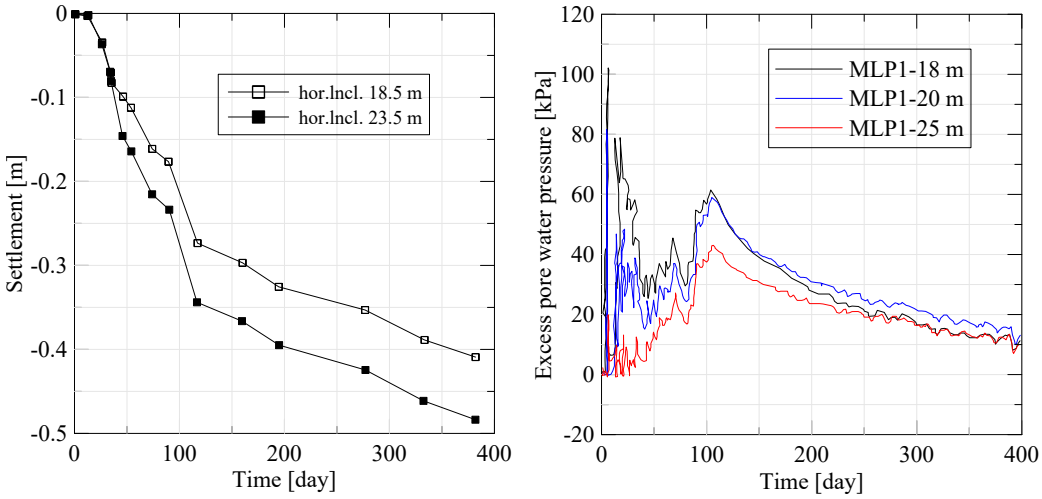

(**a**) (**b**)

Figure 7. Field measurement in Klagenfurt Project. (**a**) vertical displacements at surface; (**b**) excess pore water pressures.

4. Results

4.1. Installation Stage (2D Model)

The vertical, radial, and hoop (circumferential) (σ'_z, σ'_r, σ'_θ) stresses may still be considered the principal stresses, as the shear stresses are negligible [17]. The variation of effective stress (σ'_r, σ'_θ, σ'_z) and the mean effective stress (p') as a function of normalised distance (r/D_c) for two different layers at the end of the consolidation after 6.5 days of installation are shown in Figure 8. The logarithmic scale for the distance amplifies the zone of interest near the column.

The installation process, which includes applying the horizontal displacement that caused the soil movement and the generation of the excess pore pressure followed by the dissipation of this pressure, leads to changes in the stresses in the vicinity of the column. Based on the curves presented in Figure 8, it is feasible to identify three zones:

- Zone 1: Near the column, where σ'_r and (p') significantly vary due to column installation. In contrast, there is a little improvement in σ'_θ, and this is only in a small zone near the column.
- Zone 2: The essential characteristic in this zone, the improvement in σ'_r continues to decrease while σ'_θ shows a slight increase. The mean effective stress p' is practically unchanged. At the end of this zone, both σ'_r and σ'_θ take values close to their initial values.
- Zone 3: All of the stresses are almost identical to their original values.

In all of these zones, the changes in the vertical stresses in the clay layer are not significant. Although the stress evolution depends on the depths, they are directly proportional to the cavity expansion degree (Δ_r) and initial vertical stress which is a function of depth.

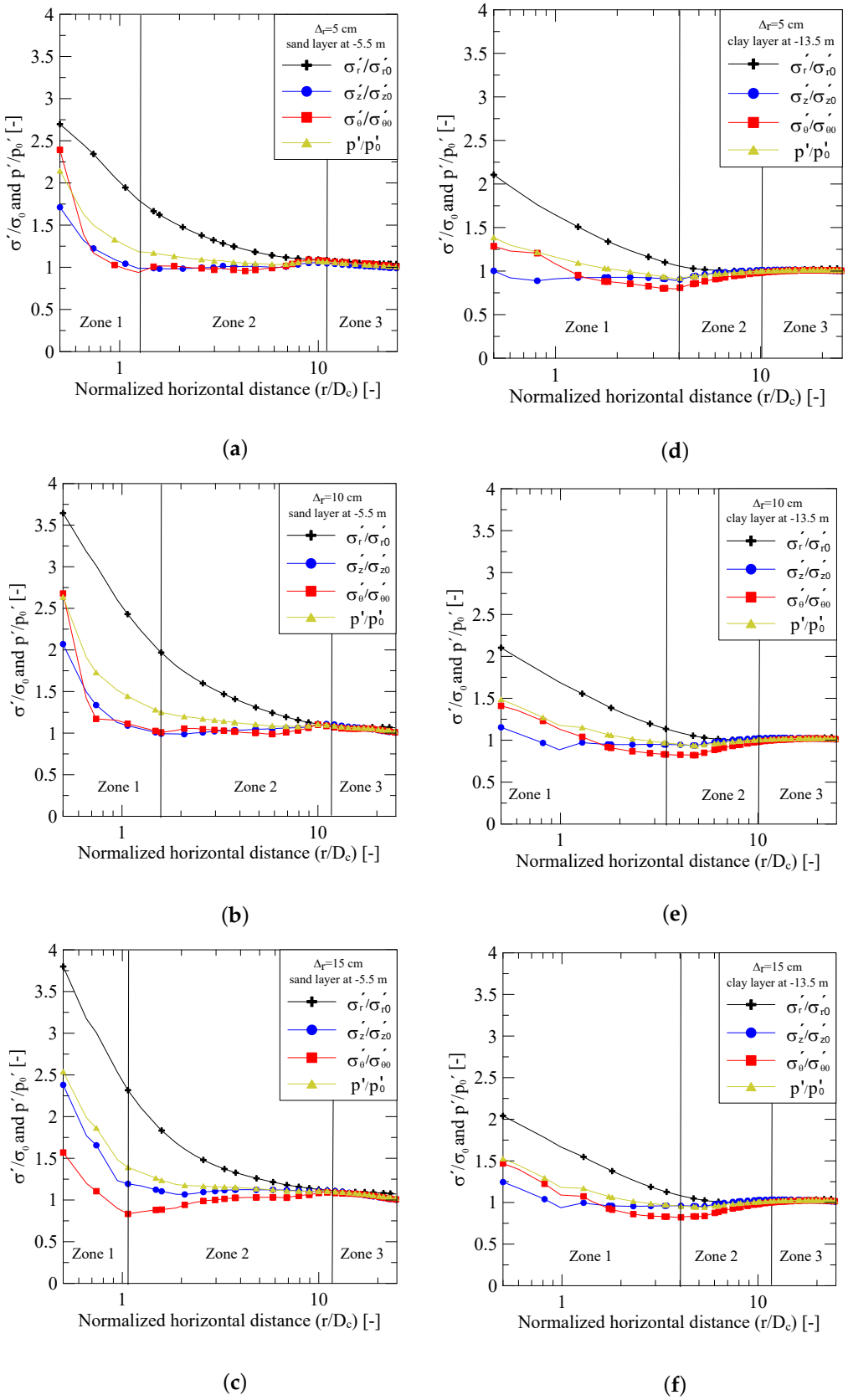

Figure 8. Stress distribution in subsoil after consolidation. (**a**) sand layer (Δ_r = 5 cm); (**b**) sand layer (Δ_r = 10 cm); (**c**) sand layer (Δ_r = 15 cm); (**d**) clay layer (Δ_r = 5 cm); (**e**) clay layer (Δ_r = 10 cm); (**f**) clay layer (Δ_r = 15 cm).

Figure 9a,b show the stress path in the $(\acute{\sigma_r}, \acute{\sigma_z})$ space plotted for two different layers at depths of -5.5 m and -12.5 m in sand and clay layers, respectively. Figure 9a,b show that the initial stresses prior to the column installation are $\sigma_z = \gamma' \cdot Z$ and $\sigma_r = \sigma_z \cdot K_0$. Therefore, the starting point for the first two stages (the stress initialization and the creation of the hole) lies on the K_0 line for both the sand and clay layers. The important change in the stresses occurs during the expansion phase, where the radial stresses increase. Different behaviours can be noticed between the sand and clay layers during the expansion phase, represented by the fluctuations of the vertical stress during this phase. These behaviours can be attributed to the dilatancy angle in the sand. The earth's pressure coefficient increases to reach the passive state during this phase. After the expansion, the prescribed displacements are removed and the dummy material is replaced by granular material, causing relaxation in the surrounding soil. The stresses in the soil fluctuate. After the complete dissipation of excess pore water pressure, the effective vertical and radial stress increases, leading to the new earth pressure coefficient between the passive state and the K_0. This range of earth pressure coefficient is similar to that observed by [23].

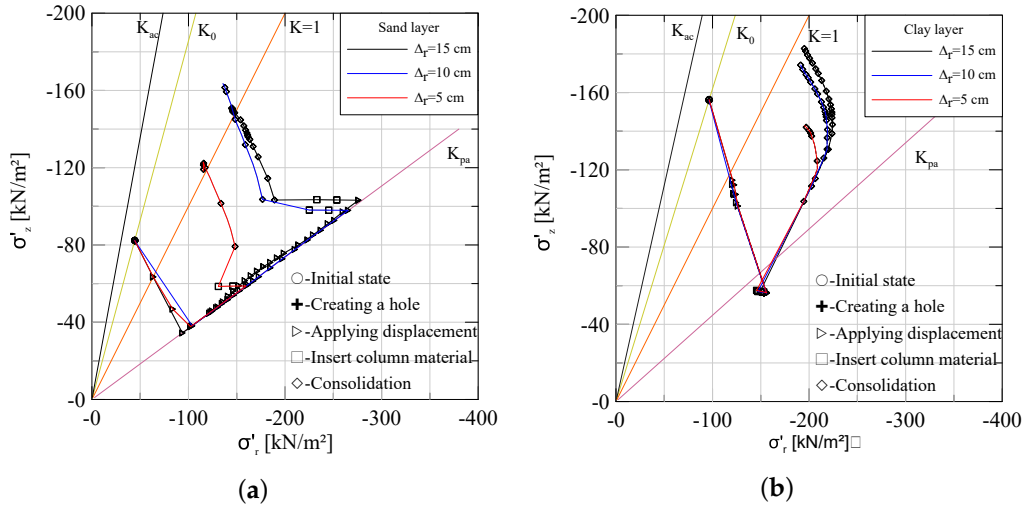

Figure 9. Stress paths for different cavity expansion in two layers at a distance of 0.4 from column axis. (**a**) sand layer; (**b**) clay layer.

The changes in stress state and stiffness after the granular column installation are different from one layer to another based on several factors, such as the soil properties and the stress level. To discuss these deviations, the distribution of the stresses at distance r_c with depth for different degrees of expansion is presented in Figure 10. As seen, a significant increase in the radial stresses σ_r' occurs in all layers, especially in sand upon the column installation. Such an increase in the radial stress is proportional to the increase in the expansion degrees. The variation of vertical stresses σ_z' due to the column installation indicate a small rise in the upper layers from their initial values where the intensity of the increase in σ_z' reduces with depth. On the other hand, there is no significant change in the circumferential stresses σ_θ'. As shown in Figure 10, the changes in stress components due to the column installation are proportional with the increase in the degree of expansion (applied prescribed displacement Δ_r).

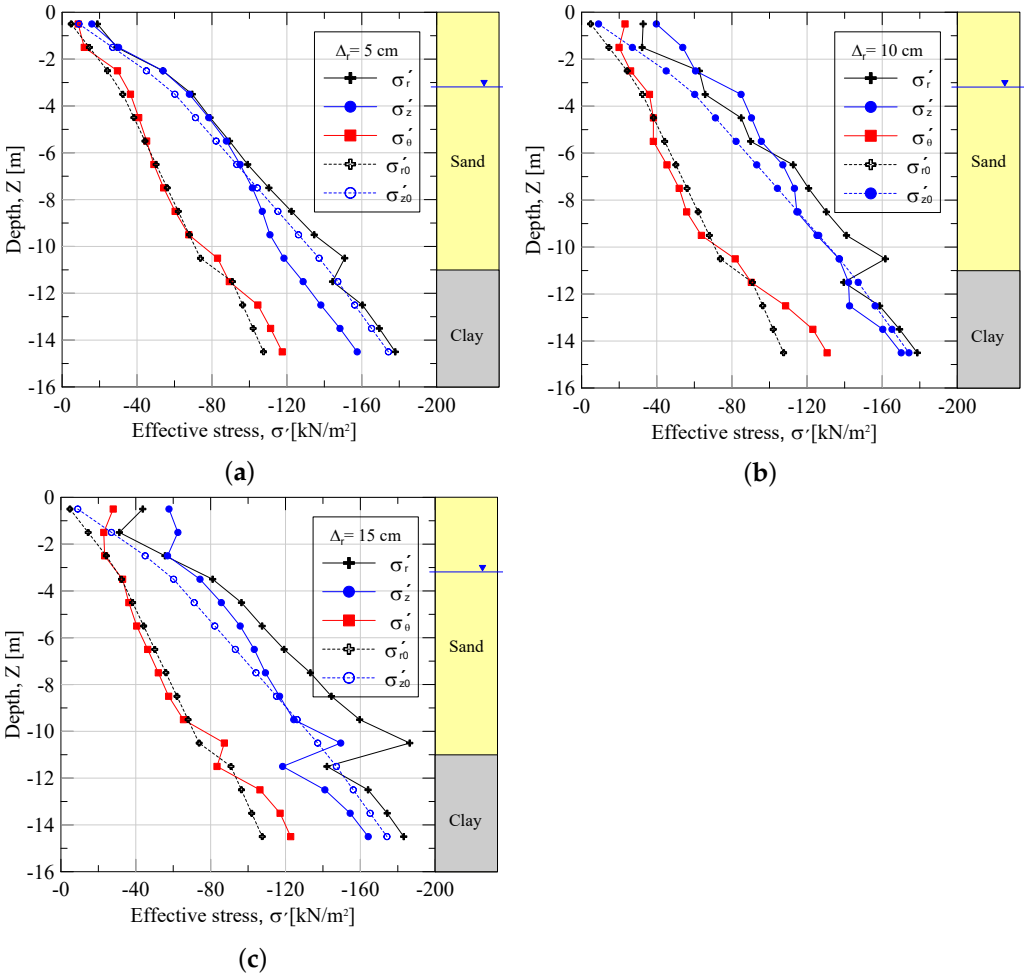

Figure 10. Stress distributions for different displacements at the distance of r_c from the column center with depths. (**a**) Δ_r = 15 cm (**b**), Δ_r = 10 cm, and (**c**) Δ_r = 15 cm.

The earth pressure coefficient is utilized to be the function that represents the change in the stresses after the installation in the surrounding area. Figure 11a,b depict the variation of K_r after consolidation in two different layers with the normalized distance to the column axis. The stress distribution is revealed by the radial earth pressure coefficients K_r:

$$K_r = \frac{\acute{\sigma_r}}{\acute{\sigma_{z0}}} \tag{3}$$

where, σ_r represents the final radial stress and σ_{z0} represents the initial vertical stress.

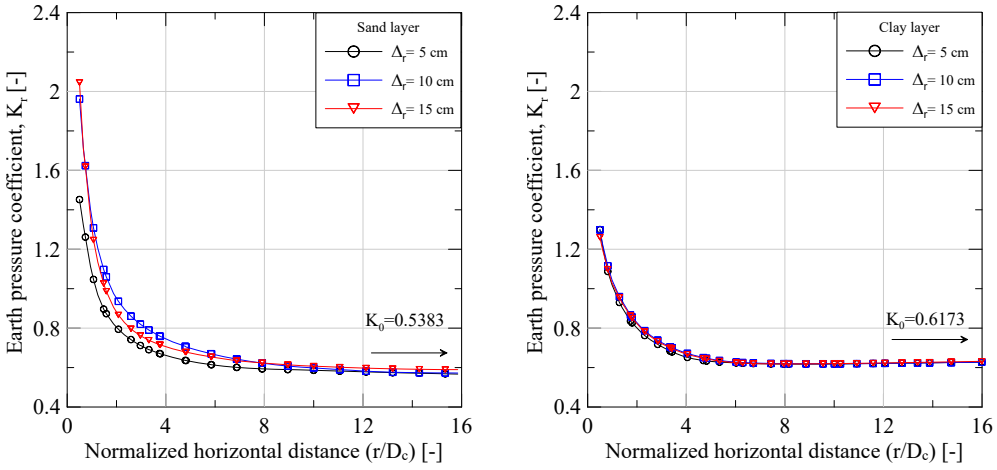

(**a**) (**b**)

Figure 11. Coefficient of earth pressure distribution after consolidation: (**a**) sand layer; (**b**) clay layer.

The radial earth pressure coefficient K_r shows significant increases from the initial value of K_0, extending to distances greater than 12 times the column diameter D_c in the sand layer, see Figure 11a, but less than six times the column diameter in the clay layer, see Figure 11b. For Δ_r = 15 cm, the sand and clay layer improvement is approximately 3.7 and 2.1 times the K_0, respectively. The figure shows that improvement in the sand is more extensive than in the clay layer, and this improvement is affected by the degree of expansion. These distributions of earth pressure coefficients are similar to those discovered by [2,5,13].

Figure 12a,b show the variation of stiffness E_{50}^{ref} and E_{oed}^{ref} with the normalised distance from the column axis for different cavity expansion degrees ($R/dot\Delta_r$) in sand and clay layers at depths of −5.5 and −12.5 m, respectively. In general, the increase in stiffness E_{50}^{ref} is affected by the expansion degree for both sand and clay layers; for example, in the sand layer in Figure 12a, the maximum enhancements in stiffness E_{50}^{ref} are 1.75, 2.05, and 2.1 times the initial values for Δ_r = 5, 10, and 15 cm, respectively, and the extent of improvement zone is approximately 10 times of the column diameter. On the other hand, the improvement in E_{oed}^{ref} is less than the improvement in E_{50}^{ref} and the improved zone extends to a distance of two times the column diameter. This behaviour is attributed to that E_{oed}^{ref} is a function of major principal stress (vertical stress, in this case). Figure 12b shows that the improvement in the clay layer is less than that seen in the sand layer, and the extent of the improvement zone is approximately eight times the column diameter; the maximum enhancements in stiffness E_{50}^{ref} are 1.5, 1.7, and 1.8 times the initial values for Δ_r = 5, 10, and 15 cm, respectively. The variation of the E_{oed}^{ref} in the clay layer shows a similar trend as shown in the sand layer. Additionally, Figure 12 illustrates the results calculated according to the equation suggested by [15] which show a drop in the stiffness value in the clay layer. This can be attributed to the dependence of the stiffness on mean effective stress p' in the calculation.

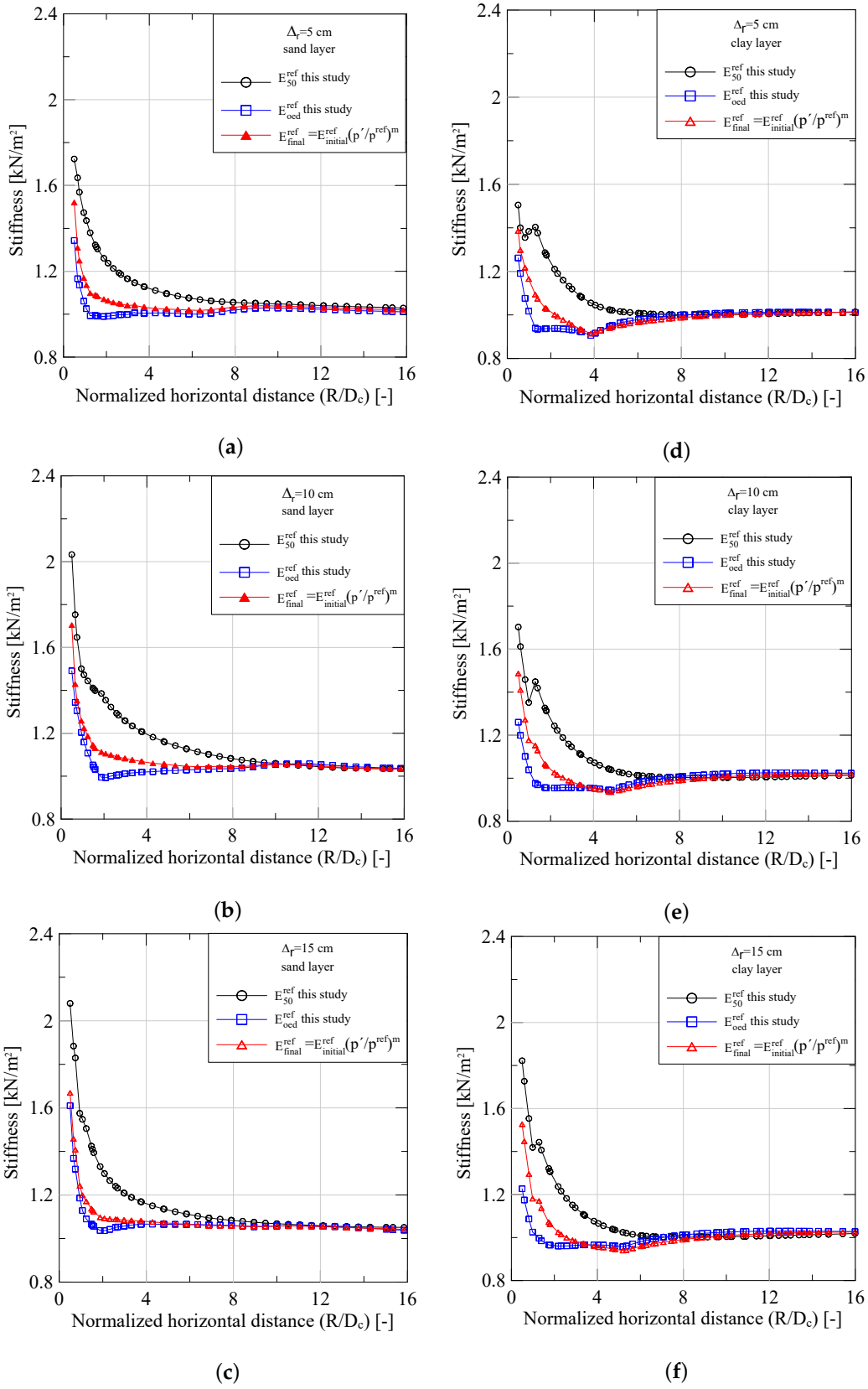

Figure 12. Variation of stiffness versus normalized distance (r/D_c) after consolidation. (**a**) sand layer (Δ_r = 5 cm); (**b**) sand layer (Δ_r = 10 cm); (**c**) sand layer (Δ_r = 15 cm); (**d**) clay layer (Δ_r = 5 cm); (**e**) clay layer (Δ_r = 10 cm); (**f**) clay layer (Δ_r = 15 cm).

The distribution of stiffness with depth at a distance of r_c from the column face is shown in Figure 13. The stiffness distribution seems to be consistent across the layers, with the exception of the fluctuation in the top portion of the sand layer owing to the large stress increment upon lateral soil displacement at low initial stress state. The effect of cavity expansion degrees on the stiffness distribution becomes clearly apparent as the cavity expansion degree increases.

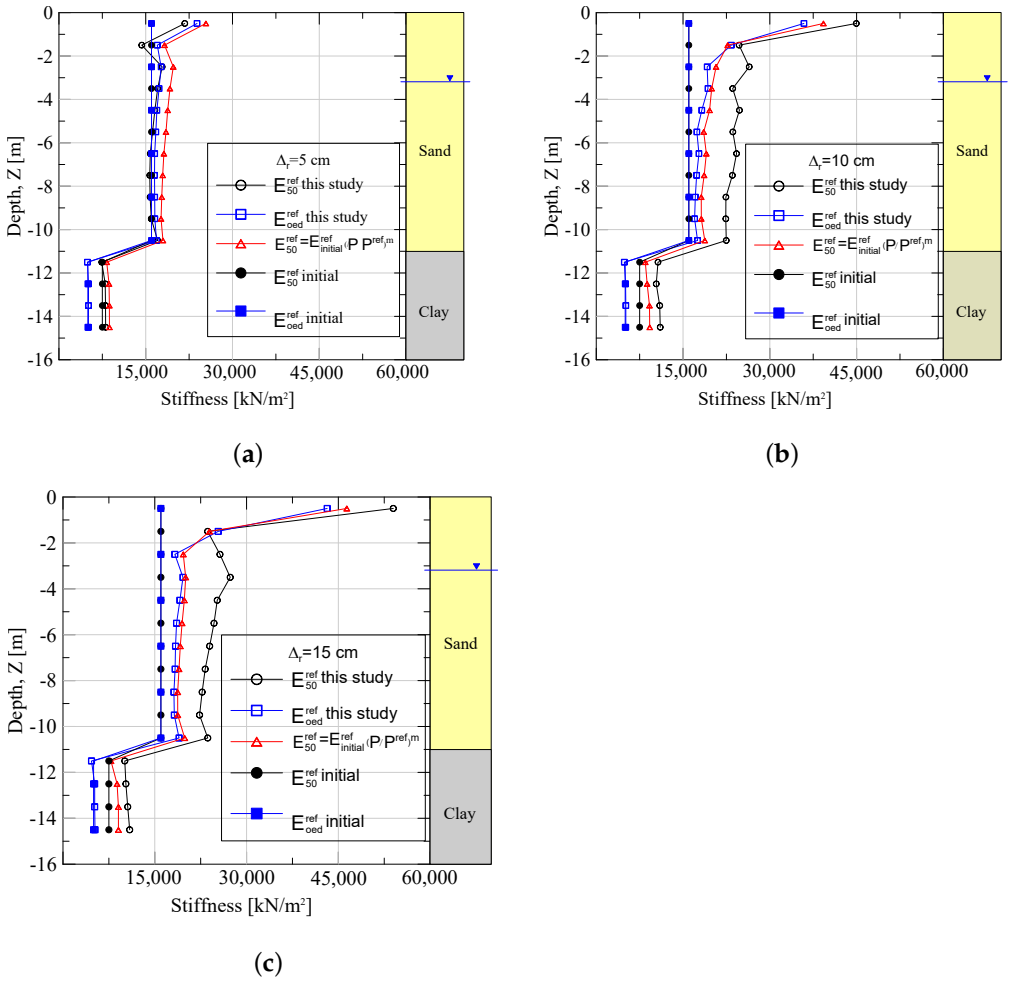

Figure 13. Variation of stiffness versus depth at distance r_c from column face. (**a**) Δ_r = 5 cm; (**b**) Δ_r = 10 cm; (**c**) Δ_r = 15 cm.

4.2. Construction Stage (3D Model)

The results of 2D models in terms of stress and stiffness are employed to generate the input parameters for the 3D construction model, following the steps explained in the methodology, which involves calculating the modified earth pressure coefficient and the modified stiffness and the average values of the updated parameters being used as initial values in the 3D model. The embankment construction is simulated in this model, and the steps of construction are considered based on the field data, see Table 1. The measurements used in this comparison obtained from multilevel piezometer, a multilevel extensometer, and horizontal inclinometers in the field. The numerical results obtained from 3D slice model for different cavity expansion degrees and measured vertical displacements versus time at the point directly beneath the centerline of the embankment are illustrated in Figure 14a,b. Apparently, as this construction model does not address the installation process, the settlement and the excess pore water pressure cannot be predicted well during the installation of the granular column, i.e., during the early construction steps of 35 days, because this stage of construction is not considered in the model. In the early stages of embankment construction, the effect of column installation on settlement is minimal (i.e., all

cavity expansion degrees provide the same settlement), and such changes are observed for settlement but only at high load levels. The increase in radial stress allows the soil to bear a more significant load and, as a result, offers better lateral support for the columns; a similar behaviour was also observed by [24]. The change in the stress regime and the stiffness due to the installation enhance the soil and give more reality to the soil's response. Therefore, the improved parameter's time vs. settlement curve results are closer to the field measurements. Both the cavity expansions of 10 cm and 15 cm seem to predict the field measurement results well. The graph also shows the settlement curve using the initial parameter of soil, which gives a higher value than the measured.

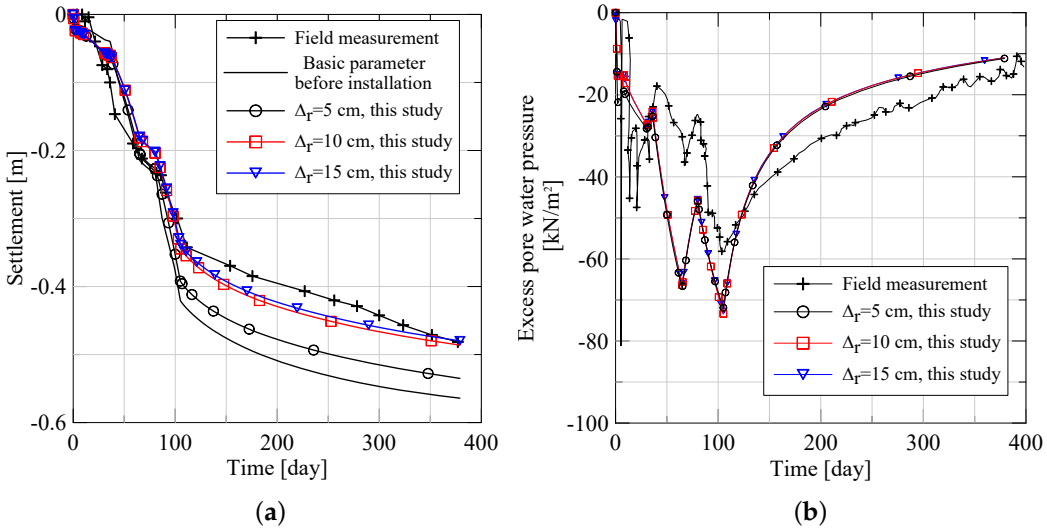

Figure 14. Comparison of the field measurement and finite element model. (**a**) settlement for different cavity expansion degrees, (**b**) excess pore pressure at 20 m.

Figure 14b shows the calculated and measured excess pore pressure at a depth of 20 m at the end of construction. The graph can be divided into two parts: the first part, which ends at 105 days, with less accurate numerical prediction, and the second part, which starts at 105 days continues until the end of monitoring time, has been better predicted. Some differences appear in the initial part of the calculated curves, but these differences disappear with time. The main reason for less accurate prediction at the first part is the direct influence of column installation that is not specifically addressed in the 3D model. However, in longer time period, the 3D provides better estimation of system behaviour. Under the embankment construction, the main factor affecting the generation of the excess pore pressure at 20 m in the untreated zone is permeability. Therefore, all the expansion degrees give almost the same results. These differences between observed and estimated excess pore water pressure may be related to the permeability change during column installation.

5. Conclusions

In this study, a numerical method was proposed to allow simulation of the granular column installation and its impact on the mechanical properties of the soil in the vicinity of column. The results obtained from present analyses showed that the procedure and methodology adopted in this study can accurately predict the change in soil due to the installation of the granular column.

- The results of the studies reveal that the lateral earth pressure coefficient, K_0, rises considerably upon the installation of the column, with average values ranging from 1.30 to 2.05 for the clay and sand layers, respectively, under different expansion degrees.
- The improvement zone around the installed granular columns extends to a maximum distance of approximately 6 to 10 times the column diameter (D_c), where the lateral pressure coefficients for the clay and sand layers are favourably influenced.

- In addition, the results show that the final radial earth pressure coefficient K_r values are in the range between $K = 1$ and K_{pa}.
- The study reveals that the granular column installation process increases the surrounding soil's stiffness (E_{50}^{ref} and E_{oed}^{ref}), where the improvement value is larger than 1.2 times the original stiffness value for all cases.
- The 3D model estimation showed reasonable compliance with field measurements for both settlement and excess pore pressure.
- The expansion degrees of 10 cm and 15 cm provide similar results to the field measurements in terms of settlement.

Author Contributions: F.G.: Analysis, Writing, Editing A.A.L.: Conceptualization, Methodology, Review, Supervision T.W.: Review, Supervision, Administration of the project. All authors have read and agreed to the published version of the manuscript.

Funding: This research received no external funding. The first author gratefully acknowledges the scholarship provided by Iraqi Ministry of Higher Education and Scientific Research.

Data Availability Statement: Not applicable.

Conflicts of Interest: The authors declare no conflict of interest.

References

1. Elshazly, H.; Hafez, D.; Mossaad, M. Back-calculating vibro-installation stresses in stone-column-reinforced soils. *Proc. Inst. Civil Eng.-Ground Improv.* **2006**, *10*, 47–53. [CrossRef]
2. Kirsch, F. Vibro stone column installation and its effect on ground improvement. In Proceedings of the International Conference on Numerical Modelling of Construction Processes in Geotechnical Engineering for Urban Environment, Bochum, Germany, 23–24 March 2006; pp. 115–124.
3. Gäb, M.; Schweiger, H.; Thurner, R.; Adam, D. Field trial to investigate the performance of a floating stone column foundation. In Proceedings of the 16th European Conference on Soil Mechanics and Geotechnical Engineering "Geotechnical Engineering for Infrastructure and Development", Edinburgh, UK, 13–17 September 2015; Millpress: Bethlehem, PA, USA, 2007; pp. 1311–1316.
4. Castro, J.; Sagaseta, C. Pore pressure during stone column installation. *Proc. Inst. Civ. Eng.-Ground Improv.* **2012**, *165*, 97–109. [CrossRef]
5. Castro, J.; Karstunen, M. Numerical simulations of stone column installation. *Can. Geotech. J.* **2010**, *47*, 1127–1138. [CrossRef]
6. Priebe, H. Design of vibro replacement. *Ground Eng.* **1995**, *72*, 183–191.
7. Pitt, J.M.; Gaul, A.; Hoevelkamp, K.; White, D.J. *Highway Applications for Rammed Aggregate Piers in Iowa Soils*; Technical report, Iowa; Department of Transportation, Bureau of Research and Technology: Iowa, IA, USA, 2003.
8. Goughnour, R. Settlement of Vertically Loaded Stone Columns in Soft Ground. 1983. Available online: https://eurekamag.com/research/020/004/020004475.php (accessed on 28 April 2022).
9. Bishop, R.F.; Hill, R.; Mott, N.F. The theory of indentation and hardness tests. *Proc. Phys. Soc.* **1945**, *57*, 147–159. [CrossRef]
10. Guetif, Z.; Bouassida, M.; Debats, J.M. Improved soft clay characteristics due to stone column installation. *Comput. Geotech.* **2007**, *34*, 104–111. [CrossRef]
11. Sexton, B.; McCabe, B. A method of modelling stone column installation for use in conjunction with unit cell analyses. In Proceedings of the International Conference on Installation Effects in Geotechnical Engineering, Rotterdam, The Netherlands, 24–27 March 2013; p. 50.
12. Al Ammari, K.; Clarke, B.G. Effect of vibro stone-column installation on the performance of reinforced soil. *J. Geotech. Geoenviron. Eng.* **2018**, *144*, 04018056. [CrossRef]
13. Shien, N.K. Cavity expansion approach in modelling stone column installation effect. *Int. J. Adv. Eng. Sci. Technol.* **2013**, *2*, 252–260.
14. Al Ammari, K.; Clarke, B. Predicting the effect of vibro stone column installation on performance of reinforced foundations. *Int. J. Civ. Environ. Struct. Constr. Archit. Eng. World Acad. Sci. Eng. Technol.* **2016**, *10*, 111–117.
15. Biarez, J.; Gambin, M.; Gomes-Correia, A.; Flavigny, E.; Branque, D. Using pressuremeter to obtain parameters to elastic-plastic models for sands. In Proceedings of the Geotechnical Site Characterization, Atlanta, GA, USA, 9–22 April 1998; pp. 747–752.
16. Gäb, M.; Schweiger, H.F.; Kamrat-Pietraszewska, D.; Karstunen, M. Numerical analysis of a floating stone column foundation using different constitutive models. In Proceedings of the 2nd International Workshop on Geotechnics of Soft Soils, Glasgow, UK, 3–5 September 2008; pp. 137–142.
17. Castro, J.; Karstunen, M.; Sivasithamparam, N. Influence of stone column installation on settlement reduction. *Comput. Geotech.* **2014**, *59*, 87–97. [CrossRef]
18. Sexton, B.G.; McCabe, B.A. Modeling stone column installation in an elasto-viscoplastic soil. *Int. J. Geotech. Eng.* **2015**, *9*, 500–512. [CrossRef]

19. Schanz, T. Formulation and verification of the Hardening-Soil Model. In *RBJ Brinkgreve, Beyond 2000 in Computational Geotechnics*; CRC Press: Boca Raton, FL, USA, 1999; pp. 281–290.
20. Jaky, J. The coefficient of earth pressure at rest. *J. Soc. Hung. Archit. Eng.* **1944**, *78*, 355–358.
21. Egan, D.; Scott, W.; McCabe, B. Installation effects of vibro replacement stone columns in soft clay. In Proceedings of the Proceedings of the 2nd International Workshop on the Geotechnics of Soft Soils, Glasgow, UK, 3–5 September 2008; pp. 23–30.
22. Adam, D.; Schweiger, H.; Markiewicz, R.; Knabe, T. Euro 2008 Stadium Klagenfurt-Prediction, Monitoring and Back Calculation of Settlement Behaviour. In *From Research to Design in European Practice*; Slovak University of Technology: Bratislava, Slovakia, 2010; pp. 217–230.
23. Watts, K.S.; Johnson, D.; Wood, L.A.; Saadi, A. An instrumented trial of vibro ground treatment supporting strip foundations in a variable fill. *Géotechnique* **2000**, *50*, 699–708. [CrossRef]
24. Schweiger, H.; Pande, G. Numerical analysis of stone column supported foundations. *Comput. Geotech.* **1986**, *2*, 347–372. [CrossRef]